

AD-A049 848

OHIO STATE UNIV RESEARCH FOUNDATION COLUMBUS

F/G 11/6

ALLOY CORROSION-FUNDAMENTAL STUDIES OF DISSOLUTION AND PASSIVIT--ETC(U)

DEC 77 J B LUMSDEN, R W STAEHLE

N00014-75-C-0665

UNCLASSIFIED

OSURF-784131-2

NL

| OF |  
AD  
A049848



AD A 049848

**the  
ohio  
state  
university**

**research foundation**

1314 kinnear road  
columbus, ohio  
43212

ALLOY CORROSION - FUNDAMENTAL STUDIES  
OF DISSOLUTION AND PASSIVITY  
OF ALLOYS AND COMPOUNDS

Roger W. Staehle and Jesse B. Lumsden  
Department of Metallurgical Engineering

For the Period  
March 1, 1976 - February 28, 1977

DEPARTMENT OF THE NAVY  
Office of Naval Research  
Arlington, Virginia 22217

Contract No. N00014-75-C-0665

December 5, 1977

**OSU**

The Ohio State University

RF Project 760233  
Interim Report

DDC  
RECEIVED  
FEB 13 1978  
A

DISTRIBUTION STATEMENT A  
Approved for public release  
Distribution Unlimited

UNCLASSIFIED

SECURITY CLASSIFICATION OF THIS PAGE (When Data Entered)

REPORT DOCUMENTATION PAGE		READ INSTRUCTIONS BEFORE COMPLETING FORM
1. REPORT NUMBER	2. GOVT ACCESSION NO.	3. RECIPIENT'S CATALOG NUMBER
4. TITLE (and Subtitle) ALLOY CORROSION - FUNDAMENTAL STUDIES OF DISSOLUTION AND PASSIVITY OF ALLOYS AND COMPOUNDS.		5. TYPE OF REPORT & PERIOD COVERED Interim Report 1/3/76 through 28/2/77
7. AUTHOR(s) J. B. Lumsden R. W. Staehle		6. PERFORMING ORG. REPORT NUMBER 14 OSUAF-784131-2 8. CONTRACT OR GRANT NUMBER(s) 15 N00014-75-C-0665
9. PERFORMING ORGANIZATION NAME AND ADDRESS The Ohio State University Research Foundation 1314 Kinnear Road Columbus, Ohio 43212		10. PROGRAM ELEMENT, PROJECT, TASK AREA & WORK UNIT NUMBERS NR 036-085/1-3-75 (471)
11. CONTROLLING OFFICE NAME AND ADDRESS Office of Naval Research Code N00014 Department of the Navy Arlington, VA 2217		12. REPORT DATE November 1977
14. MONITORING AGENCY NAME & ADDRESS (if different from Controlling Office) Office of Naval Research Resident Representative The Ohio State University Research Center 1314 Kinnear Road Columbus, OH 43212		13. NUMBER OF PAGES 25
		15. SECURITY CLASS. (of this report) Unclassified
15a. DECLASSIFICATION/DOWNGRADING SCHEDULE		
16. DISTRIBUTION STATEMENT (of this Report) Reproduction in whole or in part is permitted for any purpose of the United States Government 11 5 Dec 77		
DISTRIBUTION STATEMENT A Approved for public release; Distribution Unlimited		
17. DISTRIBUTION STATEMENT (of the abstract entered in Block 20, if different from Report) 10 Jesse B. Lumsden Roger W. Staehle 9 Interim rept. 1 Mar 76 - 28 Feb 77		
18. SUPPLEMENTARY NOTES 12 33p.		
19. KEY WORDS (Continue on reverse side if necessary and identify by block number) Corrosion Passivity Iron Films Silicon		
20. ABSTRACT (Continue on reverse side if necessary and identify by block number) The effects of Si additions to Fe on the stability of the passive film have been investigated over the pH range from 0 to 10. Silicon, in concentrations below 14.5% decreased the stability of the film. In sulfate solutions the passive current density was up to an order of magnitude less for the Fe-14.5 Si alloy relative to the Fe-8 Si alloy; the active peak decreased three orders of magnitude. In 0.1 N HCl, Fe-14.5 Si had a passive region. There was no passive zone for Fe, Fe-3 Si, or Fe-8 Si alloys in this solution. Surface		



20 Cont.

→ analysis techniques indicate that the abrupt change in stability with the addition of 14.5% Si is not the result of an  $\text{SiO}_2$  film on the surface. ↗



FUNDAMENTAL STUDIES OF DISSOLUTION  
AND PASSIVITY OF ALLOYS AND COMPOUNDS

Research Program for the  
Office of Naval Research

Contract # N00014-75-C-0665 (NR036-085)

Report of Work During the Period  
1 March 1976 - 28 February 1977

J. B. Lumsden  
R. W. Staehle

Department of Metallurgical Engineering  
The Ohio State University  
Columbus, Ohio

ACCESSION NO.	
NTIS	White Section <input checked="" type="checkbox"/>
DDI	Buff Section <input type="checkbox"/>
UNANNOUNCED	<input type="checkbox"/>
JUSTIFICATION	
<i>Letter on file</i>	
BY	
DISTRIBUTION/AVAILABILITY CODE	
Dist.	AVAIL. and SPECIAL
<i>A</i>	

Reproduction in whole or in part is permitted for  
any purpose of the United States Government

## TABLE OF CONTENTS

Abstract

Introduction . . . . . 1

Experimental . . . . . 3

Results and Discussions . . . . . 5

References . . . . . 24

# LIST OF TABLES

		<u>Page</u>
Table I	Sample Compositions	10
Table II	Open Circuit Potential (NHE)- pH Relationships (pH (pH < 7) for Sulfate Solutions	11
Table III	Passivation Potential (NHE)- pH Relationships for Sulfate Solutions	11



### FIGURE CAPTIONS

- Figure 1 The open circuit and passivation potentials (NHE) vs. silicon content in a borate buffer solution (pH = 8.4). 12
- Figure 2 The polarization curves of Fe-Si Alloys in a borate buffer solution (pH = 8.4). 13
- Figure 3 The polarization curves of Fe-Si alloys in 1N  $\text{N}_2\text{SO}_4$  (pH = 0.3) with scanning rate of 50 mv/min. 14
- Figure 4 The polarization curves of Fe-Si alloys in 1N  $\text{Na}_2\text{SO}_4$  with the pH adjusted with  $\text{N}_2\text{SO}_4$  (scanning rate 50 mv/min). 15
- Figure 5 The polarization curves of Fe-Si alloys in 1N  $\text{Na}_2\text{SO}_4$  (scanning rate 50 mv/min). 16
- Figure 6 The polarization curves of Fe-Si alloys in 1N  $\text{Na}_2\text{SO}_4$  with the pH adjusted with NaOH (scanning rate 50 mv/min). 17
- Figure 7 The polarization curve of Fe-Si alloys in 1N  $\text{Na}_2\text{SO}_4$  with the pH adjusted with NaOH (scanning rate 50 mv/min). 18
- Figure 8 The open circuit potentials and passivation potentials (NHE) vs. solution pH for Fe-Si alloys in the sulfate solutions. 19
- Figure 9 The polarization curves of Fe-Si alloys in 0.1 N NaCl solution. 20
- Figure 10 Auger analysis on a 14.5 Si sample which had been passivated for 1 hr. in 0.1 N NaCl at 200 mv (SCE). 21
- Figure 11 The passive current density and active current density vs. pH of Fe-Si alloys in the sulfate solutions. 22
- Figure 12 The passive and active current density vs. composition of Fe-Si alloys in a borate buffer solution (pH = 8.4). 23

### ABSTRACT

The effects of Si additions to Fe on the stability of the passive film have been investigated over the pH range from 0 to 10. Silicon, in concentrations below 14.5% decreased the stability of the film. In sulfate solutions the passive current density was up to an order of magnitude less for the Fe-14.5 Si alloy relative to the Fe-8 Si alloy; the active peak decreased three orders of magnitude. In 0.1 N HCl, Fe-14.5 Si had a passive region. There was no passive zone for Fe, Fe-3 Si, or Fe-8 Si alloys in this solution. Surface analysis techniques indicate that the abrupt change in stability with the addition of 14.5% Si is not the result of an  $\text{SiO}_2$  film on the surface.

## THE ELECTROCHEMICAL BEHAVIOR OF Fe - Si ALLOYS (L. Abrego)

### INTRODUCTION

High Si-Fe alloys are well known for their high degree of corrosion resistance in acid environments. Neither oxidizing nor reducing conditions affect these corrosion resistant properties. They are stable in strong acids such as  $\text{H}_2\text{SO}_4$ ,  $\text{HNO}_3$ ,  $\text{H}_3\text{PO}_4$ , and the organic acids at all concentrations and temperatures. Studies (1-3) have shown that there is a critical silicon composition of 14.5% at which a sharp increase in stability exists. Further additions of silicon do not result in a significant improvement in the corrosion resistance. A silica film resulting from the selective dissolution of iron is believed to be responsible for the stability; however, there is no direct evidence of this. Nor is there a "good" explanation rationalizing why the full protective value of this film is not reached until the alloy contains 14.5% Si.

Streicher (4) was the first to perform electrochemical studies of the effects of silicon additions to austenitic stainless steels. He found that silicon hindered both the initiation and growth of pits on 18Cr-8Ni stainless steels. These investigations were later extended by Rhodin (5) and Rhodin and Nielsen (6) who showed that the corrosion rate of 18-8 stainless steels exposed to ferric chloride decreased rapidly with the addition of silicon until the concentration was approximately 1.5%; whereupon, further additions resulted in a much slower decrease. They correlated these results with the enrichment of silicon in the film. Their analyses indicated that the silicon content of the film increased rapidly with the addition of silicon to the alloy until the amount of silicon in the alloy was approximately 1.5%, after which there was very little change in the silicon content in the film. This was the case even for alloys containing up to 4.5% silicon.



Rhodin and Nielsen obtained their results by chemical analyses on films which they isolated by dissolving the alloy in a bromine-methanol solution. The analyses of these films were later repeated by Lumsden and Staehle (7) using Auger spectroscopy to measure film compositions. Auger analysis and sputtering by argon ion bombardment were used sequentially to obtain a composition profile; silicon was not detected until well over half the film had been removed, and no enrichment was observed.

The existence of a critical silicon content in stainless steels has also been observed by Nonokshchenova et al. (8). These investigators determined the pitting potential of Fe-20Cr-20Ni-xSi alloys in 0.06N  $H_2SO_4$  + 0.04N  $NCl$ . Below 3% Si these alloys pitted; whereas, at 3% Si and above no pitting occurred. An abrupt change was also observed in the general corrosion resistance of these alloys for a silicon content between 3 and 4.5 percent, when they were exposed to acid and acid chloride solutions.

Thus silicon exerts two types of beneficial alloying effects. There is a critical concentration of 14.5% where substantial changes in the corrosion behavior of Fe-Si alloys occur, and there is a synergistic interaction with either Ni or Cr in austenitic stainless steels which reduces the critical composition approximately by a factor of five.

Finally, it has been shown that silicon has a pronounced beneficial effect on the stress corrosion behavior of stainless steels. Improvements result from the addition of silicon to both austenitic and ferritic alloys. Consequently, it is concluded that the role of silicon is more related to electrochemical effects and thus the properties of the passive film than structural effects (9, 10) of the alloys.

This work is aimed at rationalizing the role Si plays as an alloying element with respect to its influence on the composition and quality of the passive film which forms on Fe-Si in aqueous environments. Reported herein are the results of work in progress. We have repeated and extended previous electrochemical studies (11) of Fe-Si alloys. Also included are initial surface analysis studies.

## EXPERIMENTAL

### Specimen Preparation

The test samples were prepared in approximately 100 g. samples from high purity iron and silicon. Three different binary compositions were studied and Table I lists the sample fabrication history as well as the chemical analysis for each sample.

Specimens were mechanically polished and etched for metallographic examination. The iron sample was etched with a 5% Nital etch (5% nitric acid, 95% ethanol). The iron-silicon alloys were etched in a mixed acid/glycerol etch (1 part nitric, 2 parts HF, 4 parts glycerol). The iron and 14.5 Si samples had microstructures typical of ferrite solid solutions. The 3 Si and 8 Si appeared to have the barley stroke markings observed by Corson and documented by (Reiner, Marsh, and Stroughton [12]). These markings are characteristic of the etchants and etching procedure and do not suggest the presence of a second phase. The iron-silicon alloys are solid solutions of silicon in ferrite for all compositions with less than 15.3 wt % silicon. X-ray analysis also indicated single phase ferrite.

Test specimens were prepared by cutting a rectangular section of each sample. The samples were mounted in bakelite, then one end of each sample was drilled and tapped for electrical connection. The opposite face, which

was to be exposed to the electrolyte was polished through 0.05 alumina, degreased with acetone, and rinsed with distilled water before it was placed in the test cell.

Anodic polarization measurements were obtained at 25°C using a pyrex test cell. A  $\text{Hg}_2\text{SO}_4$  reference electrode was used for the sulfate solutions, while an SCE electrode was used for solutions containing chlorides. A platinum wire mesh was used as the counter electrode.

The test specimen was connected to a fluorocarbon coated stainless steel rod such that only the polished surface was exposed to the electrolyte. Electrode potentials were measured relative to the reference electrode located outside the cell and connected to the cell by an electrolyte bridge fitted with a fretted glass plug. The Lugan-Haber capillary tip of the electrolyte bridge was positioned approximately one millimeter from the sample face.

Solutions were prepared from reagent grade  $\text{Na}_2\text{SO}_4$ ,  $\text{NaCl}$ ,  $\text{Na}_2\text{B}_4\text{O}_7$  salts, reagent grade sulfuric acid and boric acid, and double distilled water. Argon gas was bubbled through the solutions 12 hrs. prior to running a test sample as well as during the polarization run. Each specimen was cathodically activated for 20 min. at a constant current density ( $60 \mu\text{A}/\text{min}$ ) to try to remove the oxide films. The sample was then allowed to attain a stationary open circuit potential before starting the polarization curve.

Potential-dynamic curves were generated using a stepwise technique starting at 100 mv below the open circuit potential and scanning at 20 mv/min in the borate solutions and at 50 mv/min in the sulfate and chloride solutions. A quasi-stationary potentiostatic approach was utilized in the  $\text{Cl}^-$  solutions where the polarization curves were generated



by changing the potential in steps of 20 mv and waiting for the current to reach a stationary value (15 min to 180 min). Each curve was repeated 2 or 3 times.

#### RESULTS AND DISCUSSION

The open circuit potential in the borate buffer are shown in Figure 1. Nagayama and Cohen (13) report the rest potential in a deaerated mixture of 0.15N  $\text{Na}_2\text{B}_2\text{O}_7$  and 0.15N boric acid, pH=8.4, as -580 mV NHE; this is only slightly more active than the -560 mV reported in this study. The addition of silicon shifted the potentials in the noble direction although the shift in the open circuit potential was not particularly dramatic. The polarization curves generated in the borate buffer are shown in Figure 2, where classic active-passive polarization behavior is exhibited by the samples. The curve generated with the Fe sample agrees with that of Nagayama and Cohen (13). A marked decrease in both the active and passive currents occurs when the Si content reaches 14.5%.

In the sulfate solutions, various pH ranges were studied. In 1N  $\text{H}_2\text{SO}_4$ , the open circuit potential for Fe was -280 mV (NHE). Crow, Meyers, and Jefferys (11) report a value of -269 mV (NHE). The difference in values may be due to the difference in deaeration techniques; the Crow, Jeffreys, Meyers study used hydrogen bubbling to deaerate their solution; whereas, this study used argon bubbling.

The polarization curves generated in the sulfate solutions are shown in Figures 3 to 7. The behavior of the iron-silicon samples in 1N  $\text{Na}_2\text{SO}_4$  with pH values of 3-14 adjusted with  $\text{H}_2\text{SO}_4$  or NaOH was examined; a solution of 1N  $\text{H}_2\text{SO}_4$  with pH=0.3 was also included in the study. Figure 8 shows the variation of the open circuit potential,  $E_p$ , with pH for each alloy

composition studied. There was no consistent influence of silicon additions on  $E_r$ . Table II lists the linear relations between  $E_r$  and pH as plotted on Figure 8 for pH < 7.

Reproducibility became a factor in the curves generated in the sulfate solution of pH = 14 (Figure 7). Such reproducibility problems in 1N NaOH have been encountered in past studies (14). The curves in the caustic pH are presented as a general indication of the behavior of the alloys in a solution of pH=14, i.e. the samples do not exhibit active-passive behavior.

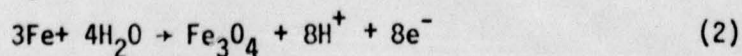
Figure 9 shows the anodic polarization curves in 0.1N NaCl solution. General dissolution occurs for the Fe, Fe-3 Si, and Fe-8 Si alloys, but a passive range is noted in the 14.5 Si sample. The active-passive transition could not be detected in the low Si samples and the Fe sample although Semino and Galvele (15) had found a narrow passive range for pure Fe in a similar solution. The difference in solution pH may account for the lack of passive behavior in the present study.

Figure 10 gives the Auger analysis of the film on the Fe-14.5 Si alloy resulting from exposure to the 0.1N NaCl solution. These results indicate that there is a slight enrichment of silicon in the film; however, the transition from general dissolution to passivity cannot be explained by the appearance of an  $\text{SiO}_2$  layer on the surface of the Fe-14.5 Si alloy. It has been generally believed that it was the existence of such a layer which produced the improved corrosion properties of the high silicon alloys.

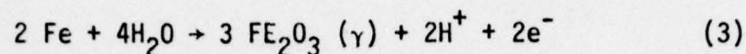
In the active region, the possible reactions occurring are:



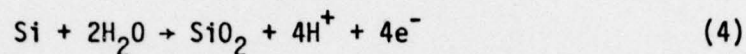
$$E_o = -0.440 + 0.029 \log (\text{Fe}^{++}) \quad (1')$$



$$E_p = -0.085 - 0.059 \text{ pH} \quad (2')$$



$$E_p = 0.221 - 0.059 \text{ pH} \quad (3')$$



$$E_p = -0.857 - 0.059 \text{ pH} \quad (4')$$

With the Fe sample reactions (1), (2), and (3) occur with reaction (3) responsible for passivation since it is in agreement with known values of passivation and activation potentials (17).

A comparison of the polarization behavior of binaries in the borate buffer and sulfate solutions shows that the effect of 3% and 8% silicon is to shift the passivation potential in the noble direction. Table II shows the linear relationships between  $E_p$  and pH for the samples in the sulfate solutions broken up into three areas, i.e.  $\text{pH} < 3$ ,  $3 < \text{pH} < 7$ ,  $\text{pH} > 7$ . A comparison of the samples of Fe, 3 Si, 8 Si shows the slopes are similar indicating similar film are forming, but the slightly higher passivation potentials of the 3 Si and 8 Si indicate that a greater amount of over potential is required to start the formation of a passive film.

These two samples are also noted for the thick porous, gel-like films that form on the surface during active dissolution prior to passivation. These films were observed by Crow, Myers, and Jeffreys (11) using 1N  $\text{H}_2\text{SO}_4$ . They observed an intense black layer which became gelatinous and separated from the sample surface at the beginning of the passive region. Similar films were observed in the present study, for higher pH values. They also noted that removing portions of the film from the surface had no apparent effect on current density; the same phenomenon was observed in this study. However, no such films formed in the borate buffer solution.

It can be postulated that the Fe oxidation reactions dominate the dissolution which occurs in the 3 Si and 8 Si. The silicon in the alloys reacts to form  $\text{SiO}_2$  but fails to form a continuous film. Figures 11 and 12



show the relation between the active current density and pH as well as the passive current density and pH in the sulfate and borate solutions, respectively. In the sulfate solutions, the low Si alloys generally give a higher current density than Fe while in the borate solutions, the low Si alloys decrease the active current density slightly, and slightly increase the passive current density.

A marked decrease in the active and passive current densities occurs at 14.5 Si as shown in Figures 11 and 12. This alloy also has a markedly different passivation potential ( $E_p$ ) and pH relationship. At 14.5%, the alloy is in the fully ordered state corresponding to  $Fe_3Si$  with silicon and iron atoms occupying definite sites in the body centered cubic superlattice formed by this alloy. All lattice sites are filled, thus reducing the reactivity of the alloy. At this composition the behavior of the alloy resembles that of silicon exhibiting little dissolution in acid solutions due to the formation of a tightly adherent and irreducible passive film. The fact that no dissolution of the sample occurred in a solution of pH = 14 (Figure 7) is due to the low kinetics of the dissolution at room temperature; a higher solution temperature might have produced greater sample dissolution.

Consideration of the fact that passivation is due to the formation of a stable oxide  $Fe_2O_3$  ( $\gamma$ ) in the low Si alloys and  $SiO_2$  in the 14.5 Si alloy, one would expect that the passivation potential should vary with pH in exactly the same way as the potential for the metal-metal oxide equilibrium value ( $E_{M/MO}$ ) such that

$$E_p = E_p^\circ - 0.059 \text{ pH} \quad (16)$$

Such a dependance however is not always the case. The discrepancy between  $E_p$  and  $E_{M/MO}$  may be due to a potential drop within the film.

#### SUMMARY

Polarization curves have been generated for iron silicon binary alloys in borate, sulfate, and sodium chloride solutions. The electrochemical behavior such as  $E_Y$  (open circuit potential) has been related to composition and pH. The passive potential has been related to pH in the sulfate solutions. Both iron oxide and silicon oxide films have been postulated as responsible for passivation in these alloys, while the stability of the 14.5 Si alloy has been related to the ordered structure of the alloy which causes its behavior to resemble that of silicon.

A limited Auger analysis has been carried out on the passive films. Results suggest that the abrupt improvement in the corrosion properties of the Fe - 14.5 Si alloy relative to the low silicon alloys is not because of the appearance of an  $SiO_2$  surface film as previously supposed.

Further work is continuing on passivation breakdown in chloride solutions, current decay curves and analysis of the composition of the films responsible for passivation in these alloys.

TABLE I

## SAMPLE COMPOSITIONS

Sample	Chemical Analysis						Fabrication History
	Fe	Si	C	Mn	P	S	
14.5 Si	85.5	14.5	-	-	-	-	Melted above 1500°C, held for 20 minutes, power turned down slowly at 1% power control every 15 min.
8 Si	92.0	8.0	-	-	-	-	Melting same as above, however power turned off and cooled from liquid in argon.
3 Si	96.42	3.45	0.027	0.075	0.005	0.018	Melted above 1500°C for 10 min., allowed to cool to room temperature in furnace.
100 Fe	99.99	0.01	-	-	-	-	Heated to 1200°C/24 hours, furnace cooled to 900°C/48 hrs., cooled at rate of 100°C/24 hrs. to 600°C and furnace cooled.



TABLE II

Open Circuit Potential (NHE) - pH Relationships (pH < 7) for Sulfate Solutions:

<u>Sample</u>	<u>Relation, E<sub>y</sub></u>
100 Fe	-0.306 - 0.039 pH
3 Si	-0.274 - 0.055 pH
8 Si	-0.301 - 0.048 pH
14.5 Si	-0.205 - 0.055 pH

TABLE III

Passivation Potential (NHE) - pH Relationships for Sulfate Solutions:

<u>Sample</u>	<u>E<sub>p</sub></u> <u>pH &lt; 3</u>	<u>E<sub>p</sub></u> <u>3 &lt; pH &lt; 7</u>	<u>E<sub>p</sub></u> <u>pH &gt; 7</u>
100 Fe	0.64 - 0.06 pH	0.29 + 0.05 pH	0.99 - 0.06 pH
3 Si	0.74 - 0.08 pH	0.32 + 0.05 pH	0.78 - 1.0 pH
8 Si	0.84 - 0.08 pH	0.39 + 0.05 pH	1.07 - 0.05 pH
14.5 Si		-0.10 - 0.02 pH	-0.45 + 0.03 pH

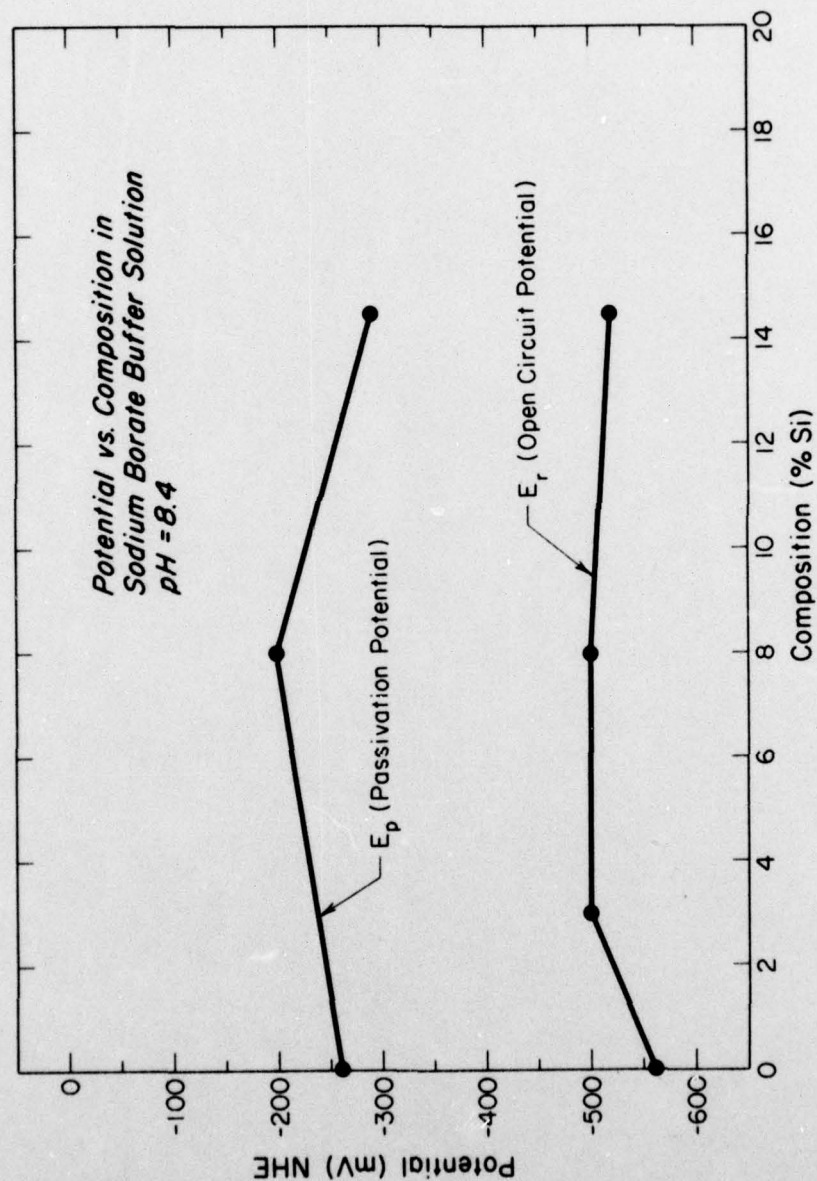


Figure 1 The open circuit and passivation potentials (NHE) vs. silicon content in a borate buffer solution (pH = 8.4).

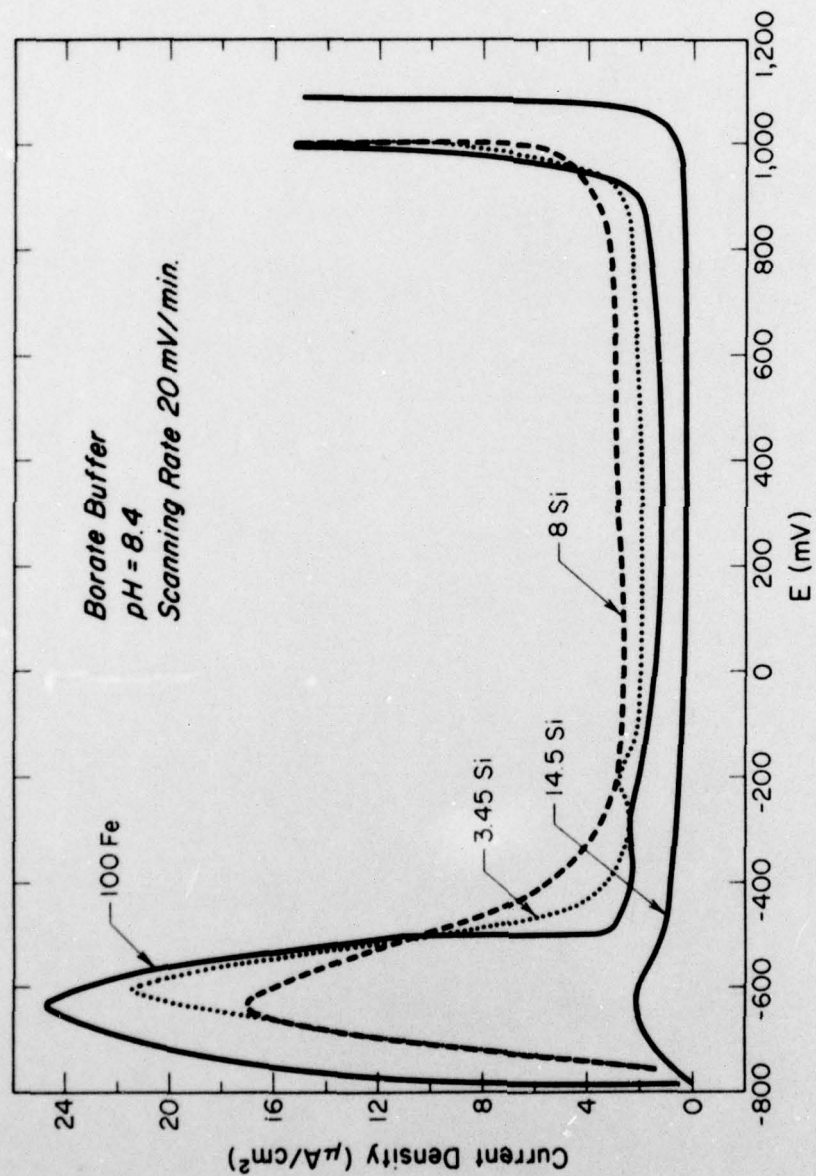


Figure 2 The polarization curves of Fe-Si Alloys in a borate buffer solution (pH = 8.4).



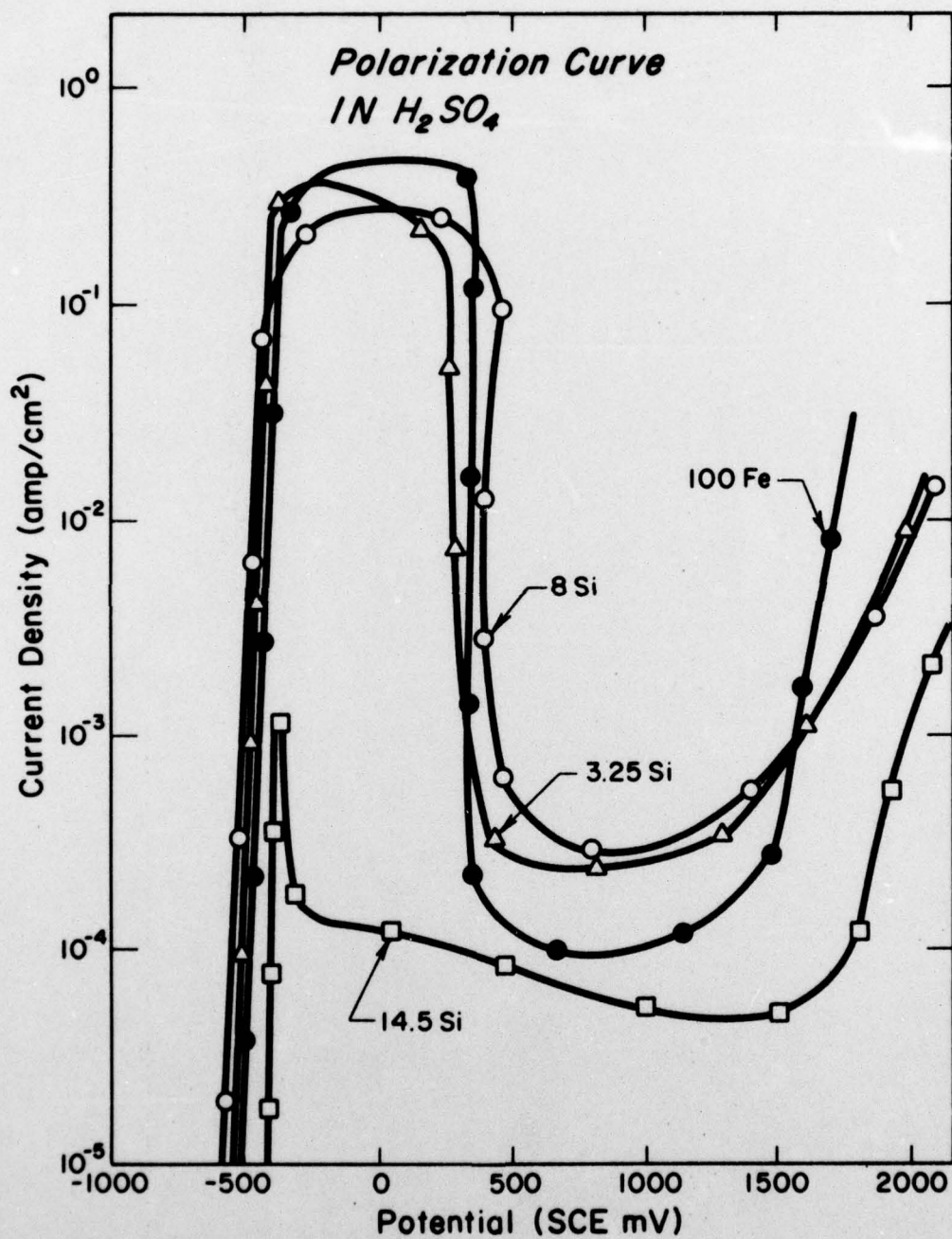


Figure 3 The polarization curves of Fe-Si alloys in 1N  $N_2SO_4$  (pH = 0.3) with scanning rate of 50 mv/min.

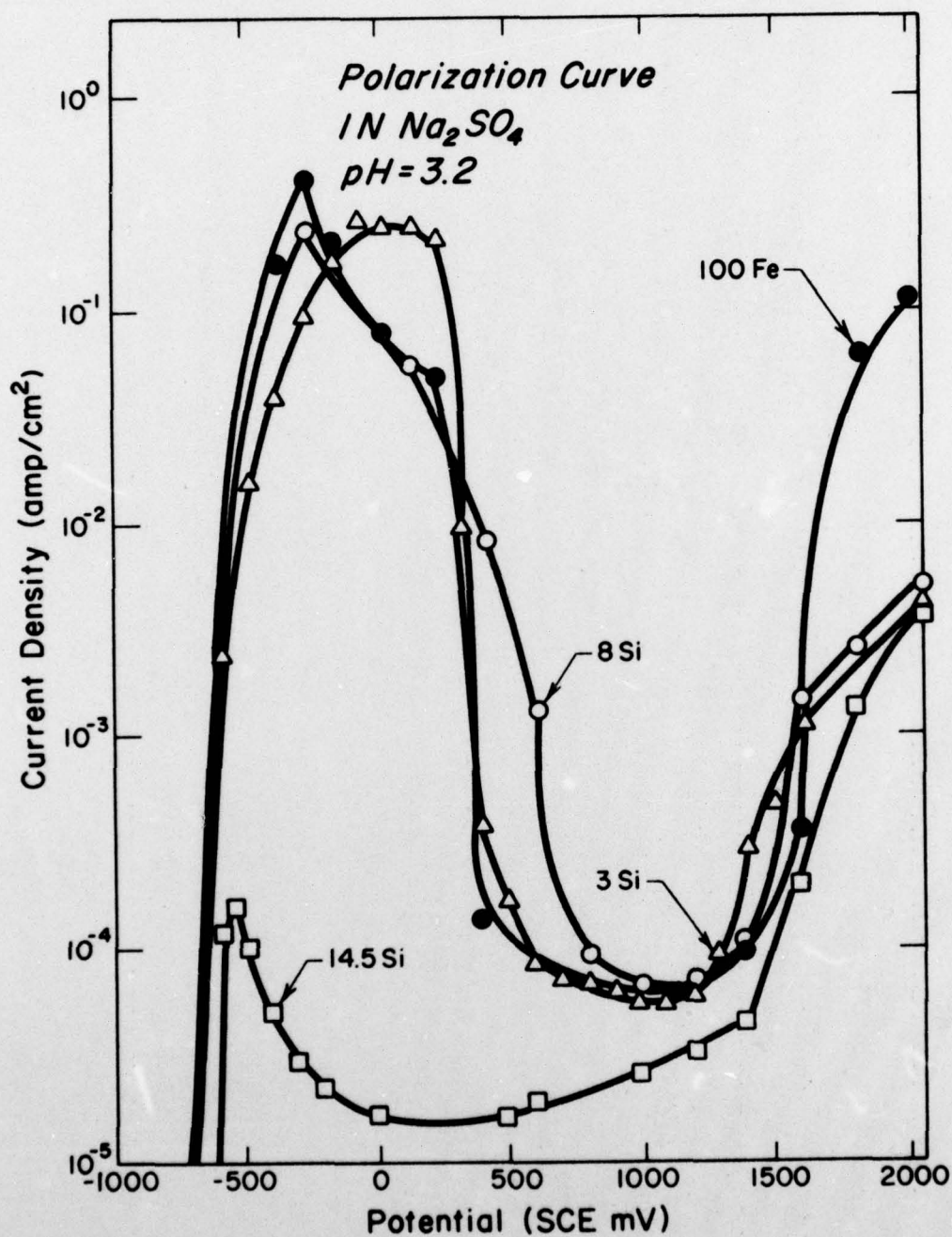


Figure 4 The polarization curves of Fe-Si alloys in 1N Na<sub>2</sub>SO<sub>4</sub> with the pH adjusted with N<sub>2</sub>SO<sub>4</sub> (scanning rate 50 mv/min).

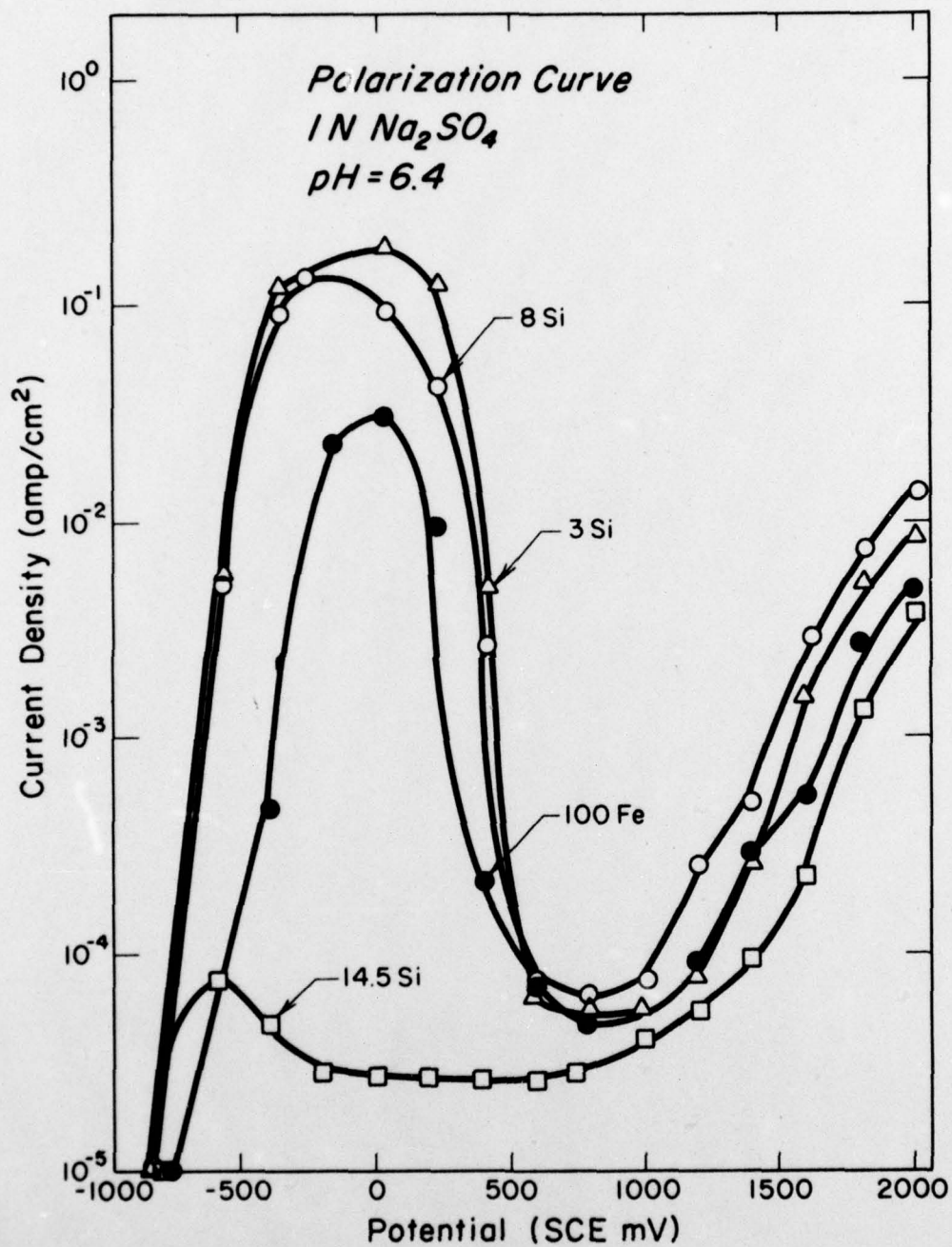


Figure 5 The polarization curves of Fe-Si alloys in 1N Na<sub>2</sub>SO<sub>4</sub> (scanning rate 50 mv/min).



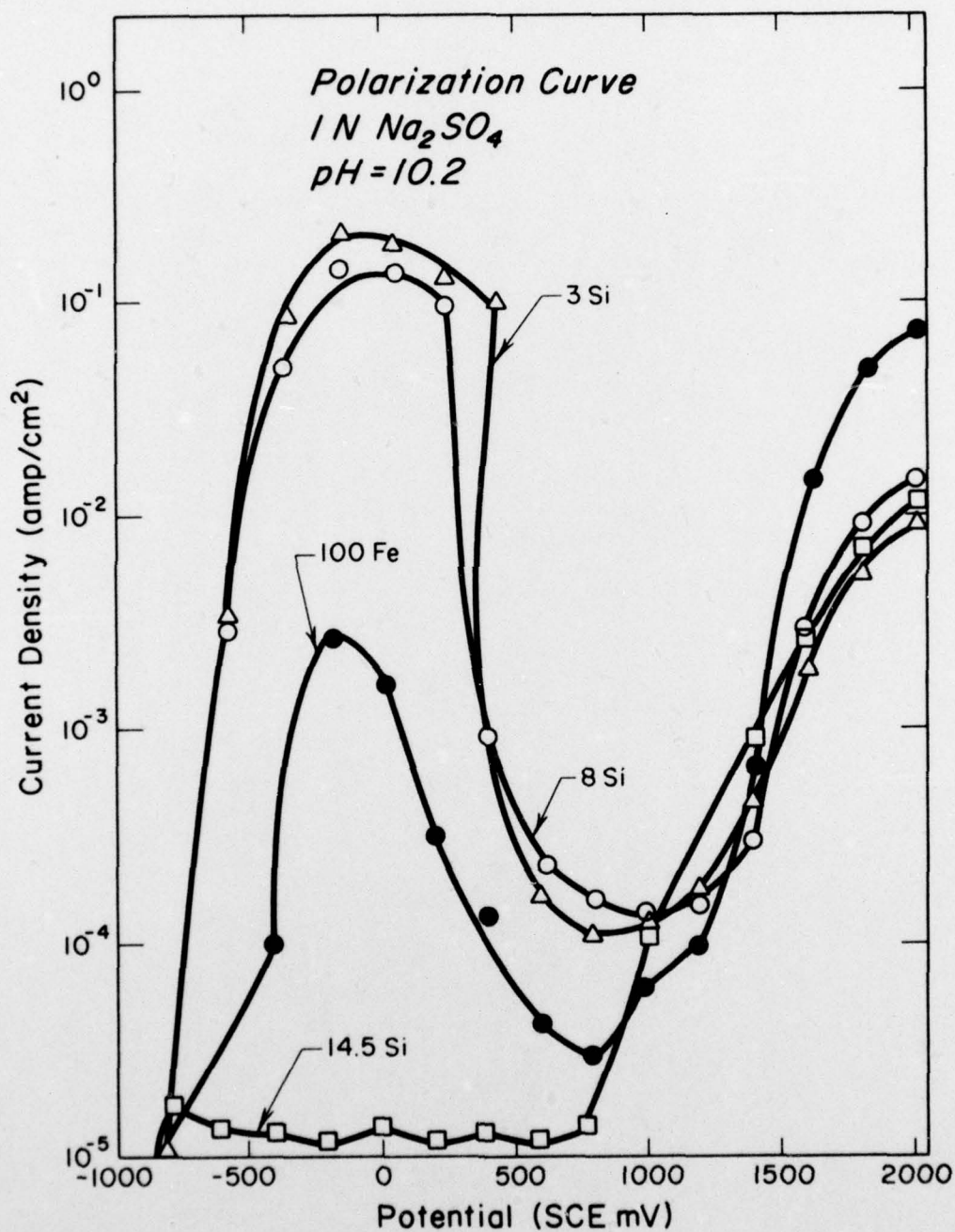


Figure 6 The polarization curves of Fe-Si alloys in 1N Na<sub>2</sub>SO<sub>4</sub> with the pH adjusted with NaOH (scanning rate 50 mv/min).

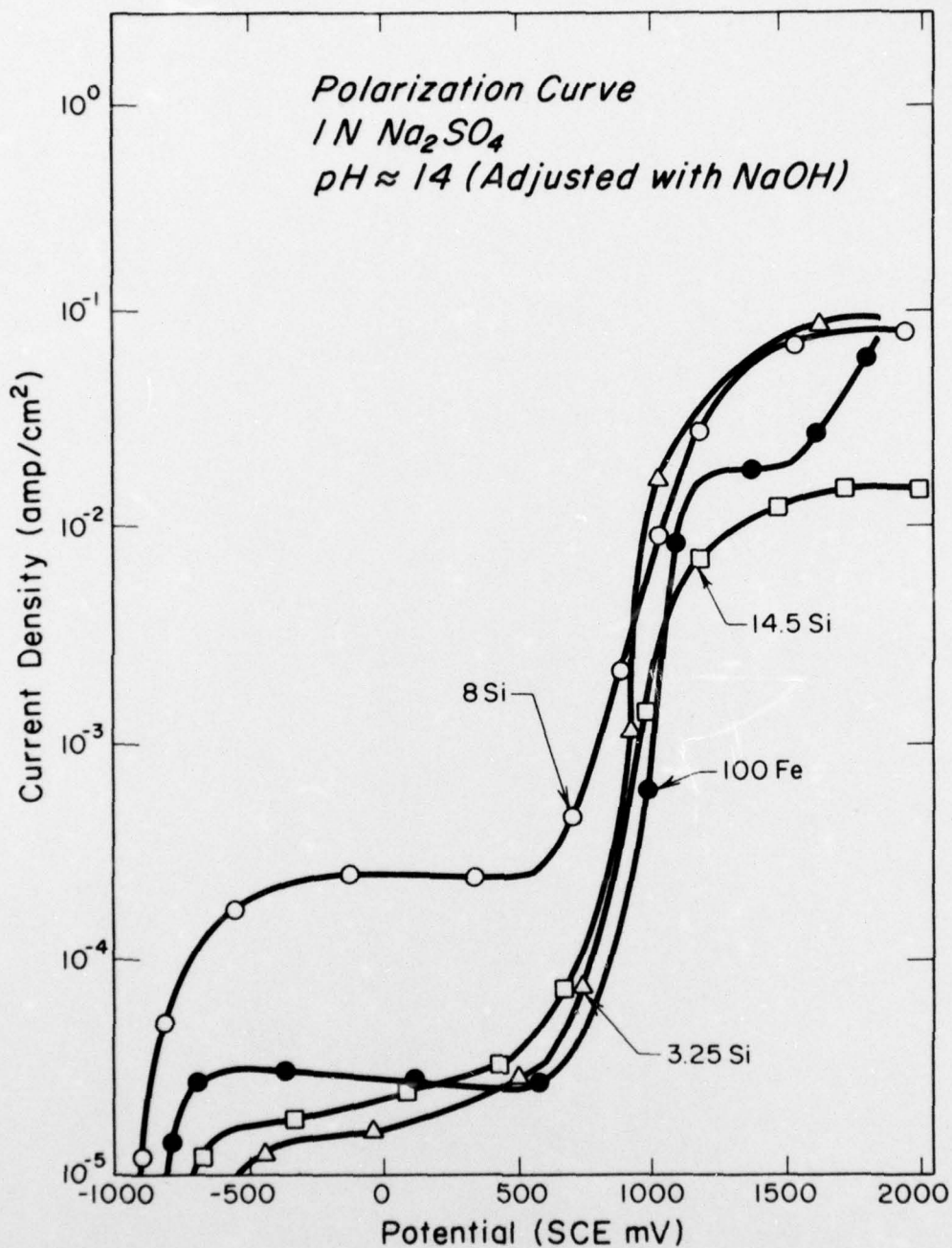


Figure 7 The polarization curve of Fe-Si alloys in 1N Na<sub>2</sub>SO<sub>4</sub> with the pH adjusted with NaOH (scanning rate 50 mv/min).

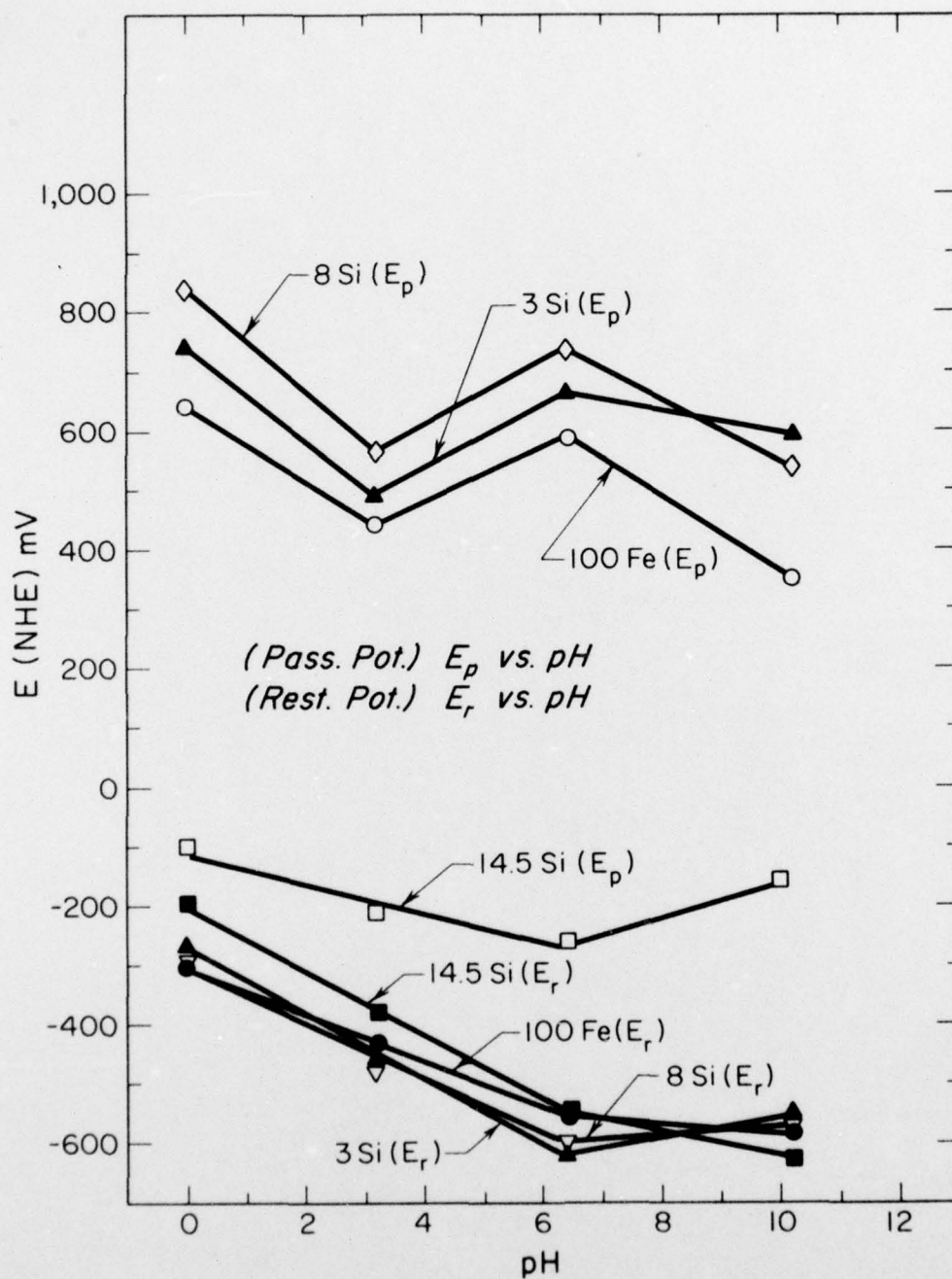


Figure 8 The open circuit potentials and passivation potentials (NHE) vs. solution pH for Fe-Si alloys in the sulfate solutions.



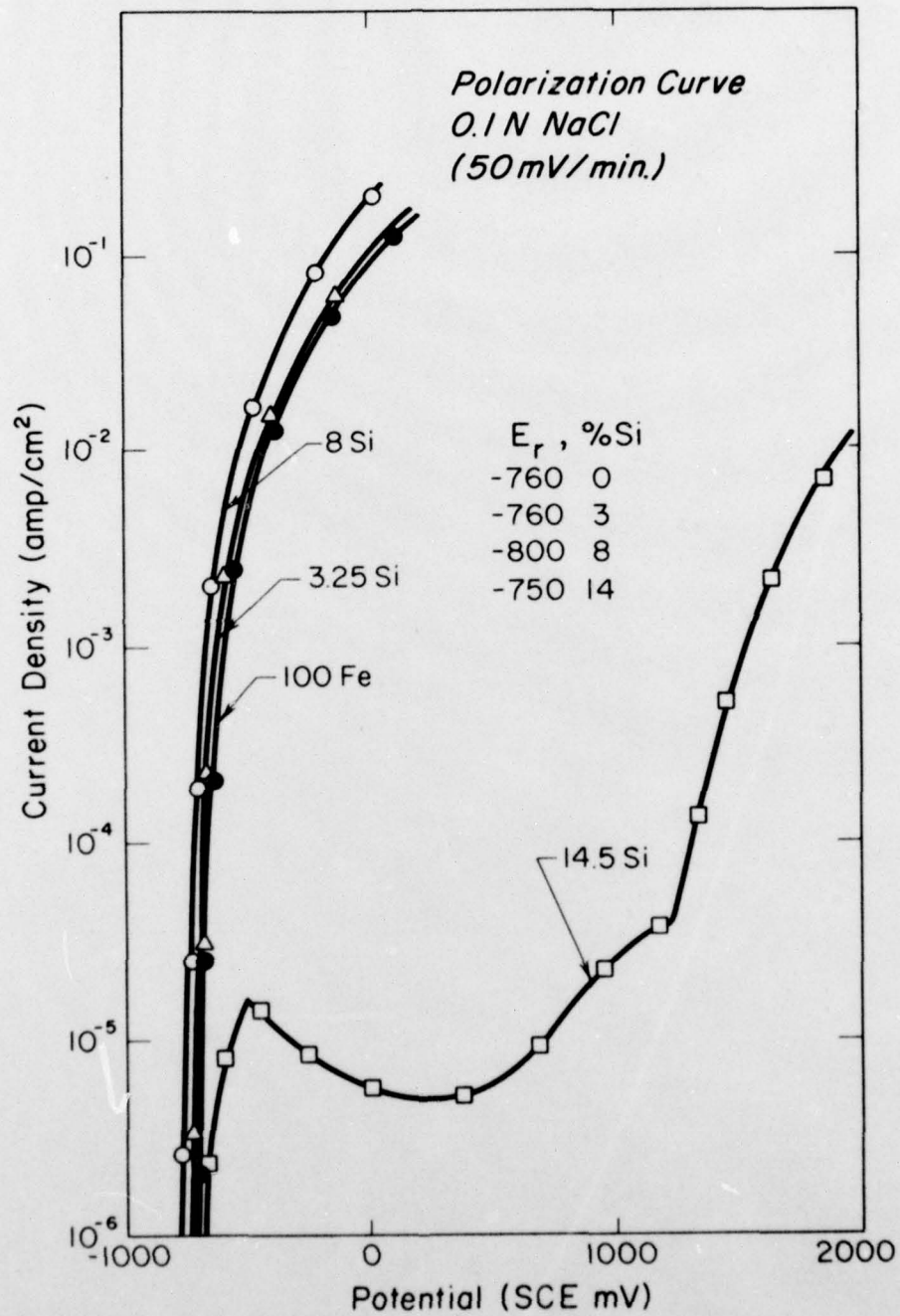


Figure 9 The polarization curves of Fe-Si alloys in 0.1 N NaCl solution.

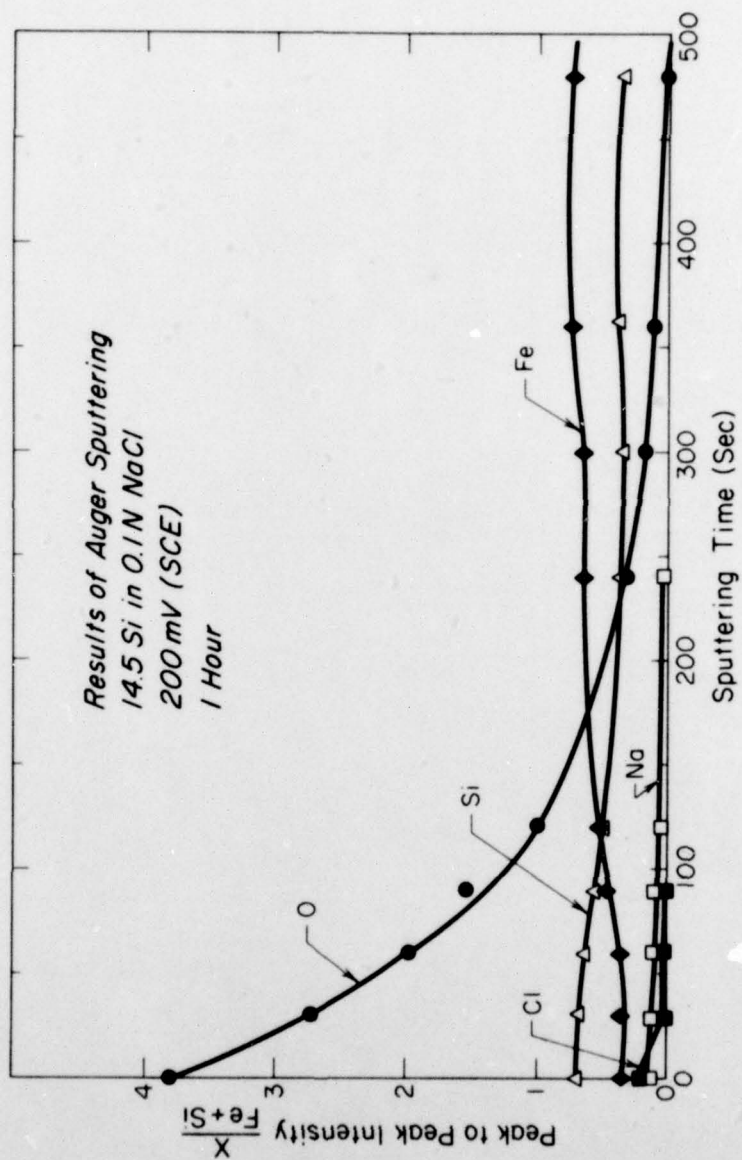


Figure 10 Auger analysis on a 14.5 Si sample which had been passivated for 1 hr. in 0.1 N NaCl at 200 mv (SCE).

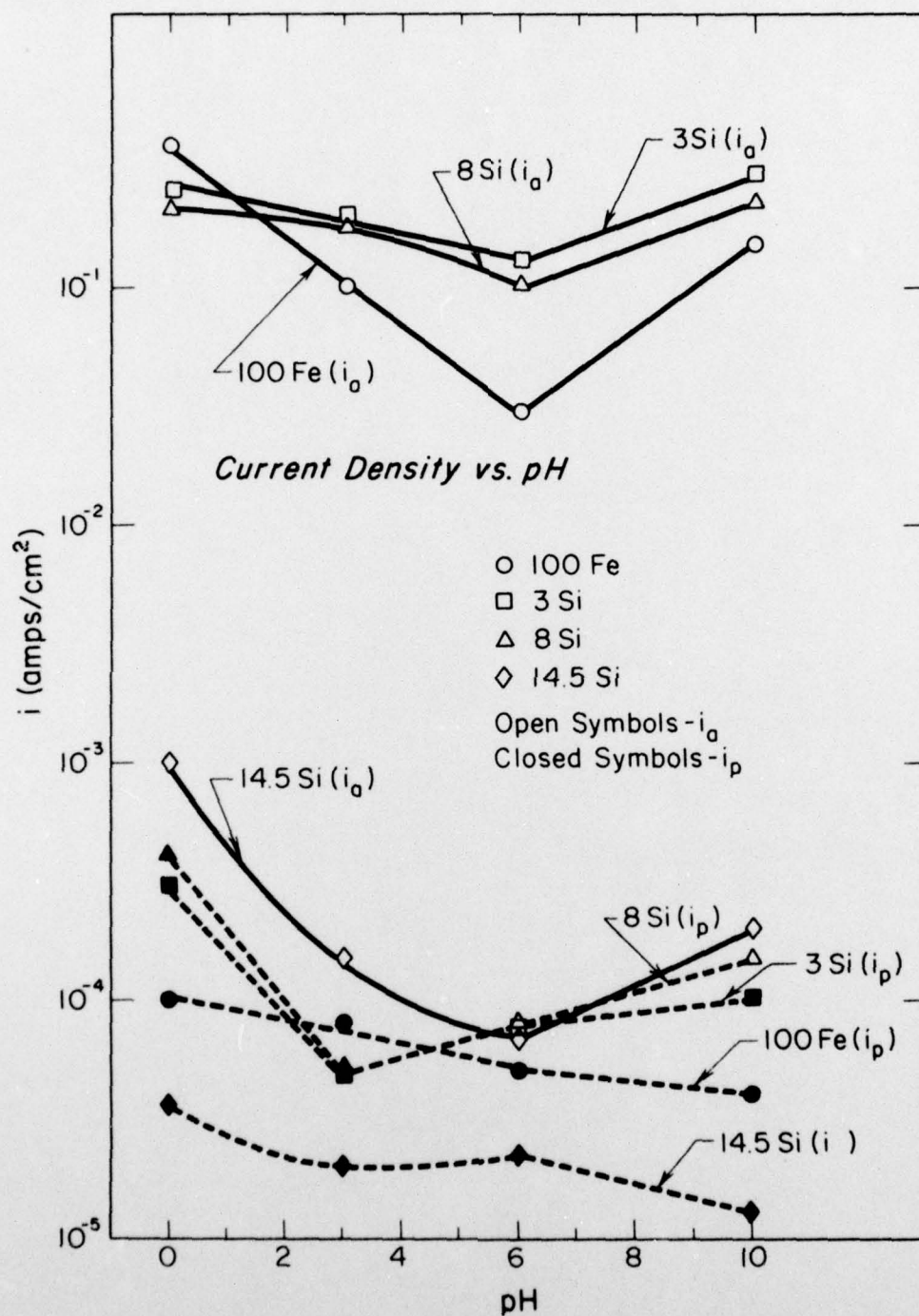


Figure 11 The passive current density and active current density vs. pH of Fe-Si alloys in the sulfate solutions.



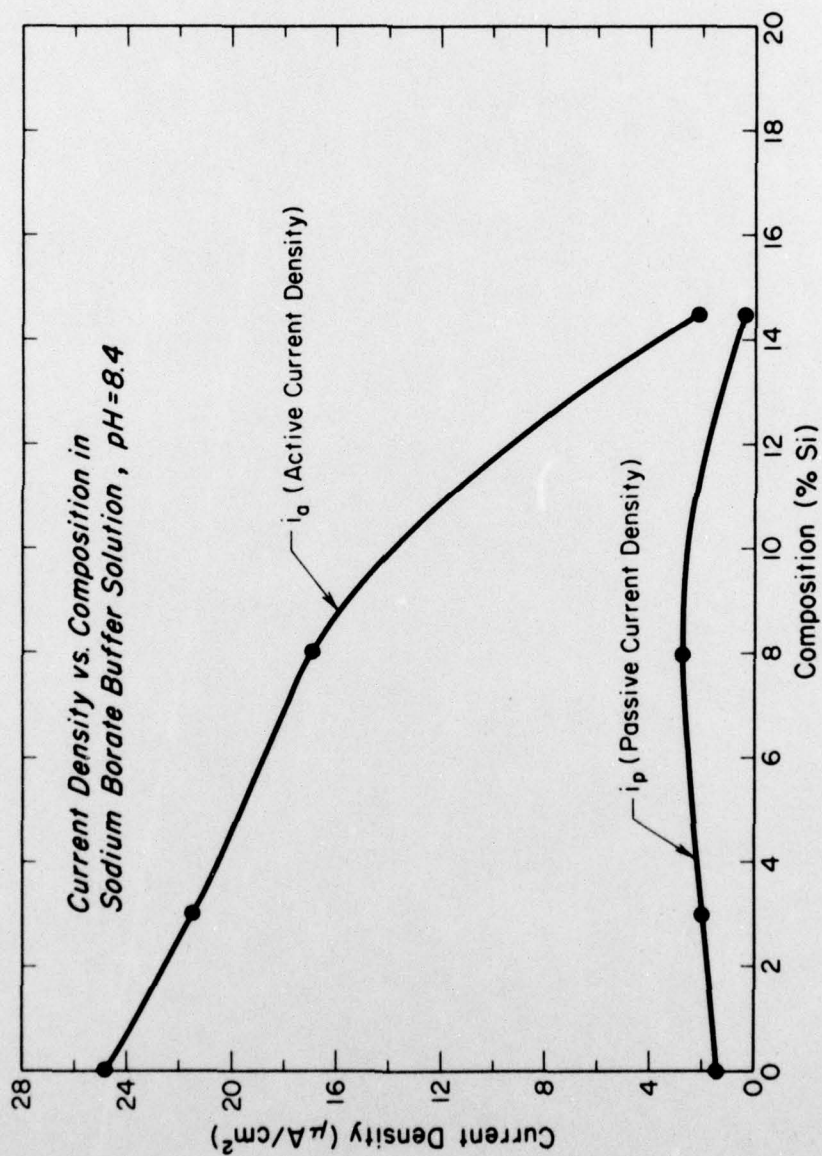


Figure 12 The passive and active current density vs. composition of Fe-Si alloys in a borate buffer solution (pH = 8.4).

## REFERENCES

1. R. J. McKay and R. Worthington, Corrosion Resistance of Metals and Alloys, Reinhold Publishing Corporation, New York, 1936, P.274.
2. H. H. Uhlig, ed., The Corrosion Handbook, John Wiley and Sons, New York, 1948, p. 201.
3. L. L. Shrier, ed. Corrosion, Vol. 1, Geo. Newnes Co., London, 1976, p. 3.120.
4. M. A. Streicher, J. Electrochem. soc., 103, 375 (1956).
5. T. N. Rhodin, Corrosion, 11, 465t (1956).
6. N. A. Nielsen and T. N. Rhodin, Z. Electrochem., 62, 707 (1958).
7. J. B. Lumsden and R. W. Staehle, Scripta Met., 6, 1205 (1972); J. B. Lumsden and R. W. Staehle, ASTM STP 596, 39 (1975).
8. S. M. Novohsherova, A. A. Babakov, and V. M. Kryazheva, Z. Metallurg., 4, 665 (1968).
9. A. W. Logirow and J. R. Bates, Corrosion 25, 15 (1969).
10. R. M. Latanision and R. W. Staehle, "Stress Corrosion Cracking of Fe-Ni-Cr Alloys," Proc. Fundamental Aspects of Stress Corrosion Cracking, p. 214 NACE, 1968.
11. W. B. Crow, J. R. Myers, and J. V. Jeffreys, Corrosion, 28, 77 (1972).
12. E. S. Greiner, J. S. Marsh, and B. Stroughton, The Alloys Iron and Silicon, McGraw-Hill Book Co., 1933, 21.
13. M. Nagayama and M. Cohen, "Anodic Oxidation of Fe in a Neutral Solution: The Nature and Composition of the Passive Film," J. Electrochemical Society, Vol. 109 (Sept. 1962), 781.
14. S. Asakura and K. Nobe, "Kinetics of Anodic Processes on Fe in Alkaline Solutions", J. Electrochemical Society, Vol. 118 (Apr. 1971), 536.

References - Cont.

15. C. J. Semino and J. R. Galvele, "Passivity Breakdown of High Purity Fe and AISI 4340 Steel in 0.5 M NaCl Solution", Corrosion Sci., Vol. 16 (1976), 297.
16. R. P. Frankenthal, "On Passivity of Iron and Its Alloys", Honolulu Conference on Passivity, Honolulu, Hawaii, Mar. 1975.
17. M. Pourbaix, Atlas of Electrochemical Equilibria in Aqueous Solutions, NACE, Houston, 1974, 461.